Supplementary information

A strength of the study was the large and varied series of glasses with differently shaped AuNP at varying concentrations. In this supplementary information document photos, transmission spectra and optical power limiting (OPL) plots are presented. The curve fitting results for the OPL data at 532 nm excitation wavelength are also given.

Table 1: Naming convention used for the different glasses in this document

AuNP doped MTEOS Glasses	
Reference	Description
AuNP-S1	MTEOS material, cc 0,25 Gold Spheres 23nm
AuNP-S2	MTEOS material, cc 0.5x Gold Spheres 23nm
AuNP-S3	MTEOS material, cc 1x Gold Spheres 23nm
AuNP-S4	MTEOS material, cc 2x Gold Spheres 23nm
AuNP-S10	MTEOS material, cc 0.125x Gold Spheres 45nm
AuNP-S11	MTEOS material, cc 0.25x Gold Spheres 45nm
AuNP-S12	MTEOS material, cc 0.5x Gold Spheres 45nm
AuNP-S13	MTEOS material, cc 1x Gold Spheres 45nm
AuNP-S14	MTEOS material, cc 2x Gold Spheres 45nm
AuNP-B31	MTEOS material, cc 0.25x Gold BiPy (plasmon around 640nm)
AuNP-B32	MTEOS material, cc 0.5x Gold BiPy (plasmon around 640nm)
AuNP-B33	MTEOS material, cc 1x Gold BiPy (plasmon around 640nm)
AuNP-B41	MTEOS material, cc 0.25x Gold BiPy (plasmon around 700nm)
AuNP-B42	MTEOS material, cc 0.5x Gold BiPy (plasmon around 700nm)
AuNP-B43	MTEOS material, cc 1x Gold BiPy (plasmon around 700nm)
AuNP-B51	MTEOS material, cc 0.25x Gold BiPy (plasmon around 770nm)
AuNP-B52	MTEOS material, cc 0.5x Gold BiPy (plasmon around 770nm)
AuNP-B53	MTEOS material, cc 1x Gold BiPy (plasmon around 770nm)
Pure MTEOS	MTEOS material (without AuNPs)

Photos

The photos show the good optical quality of the glasses.

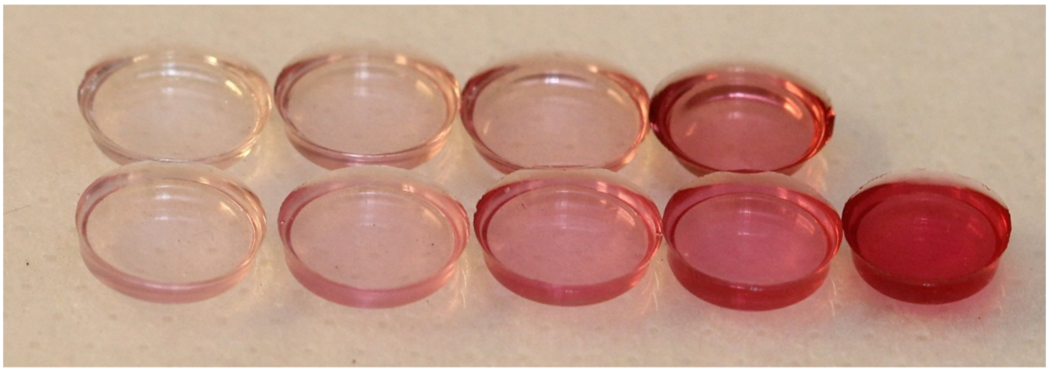

Crude MTEOS glass materials, AuNP-S1 – AuNP-S4 (top) and AuNP-S10 – AuNP-S14 (Bottom)

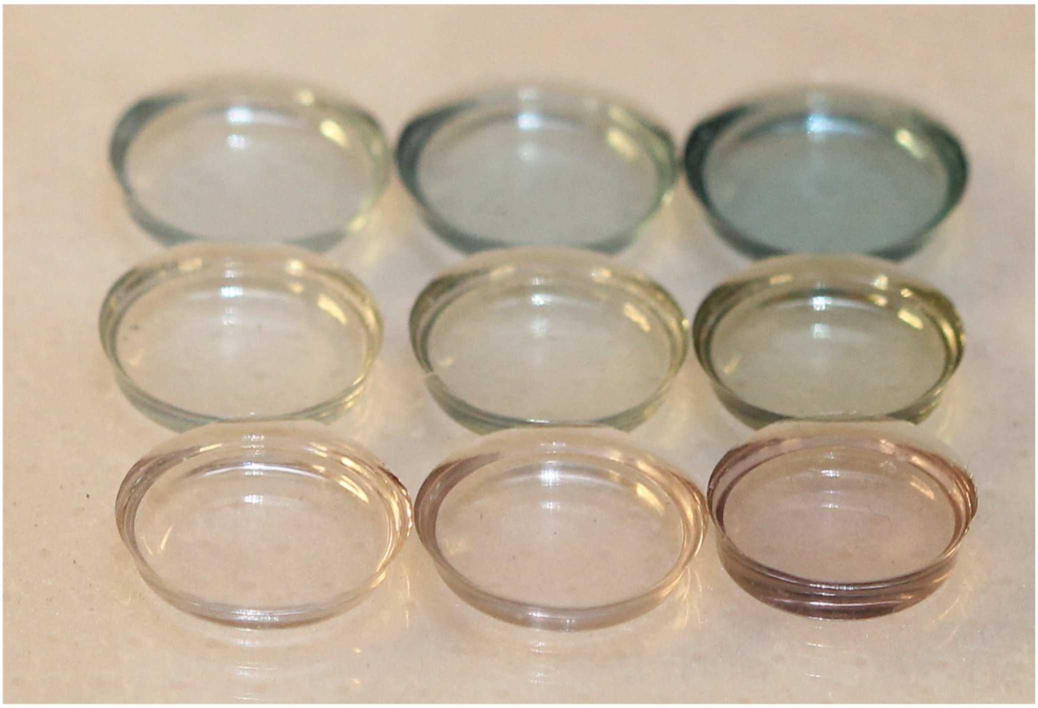

Crude MTEOS glass materials, AuNP-B31 – AuNP-B33 (top), AuNP-B41 – AuNP-B43 (middle) and AuNP-B51 – AuNP-B53 (bottom)

All glass materials were cut and polished to a thickness of 1± 0.05 mm.

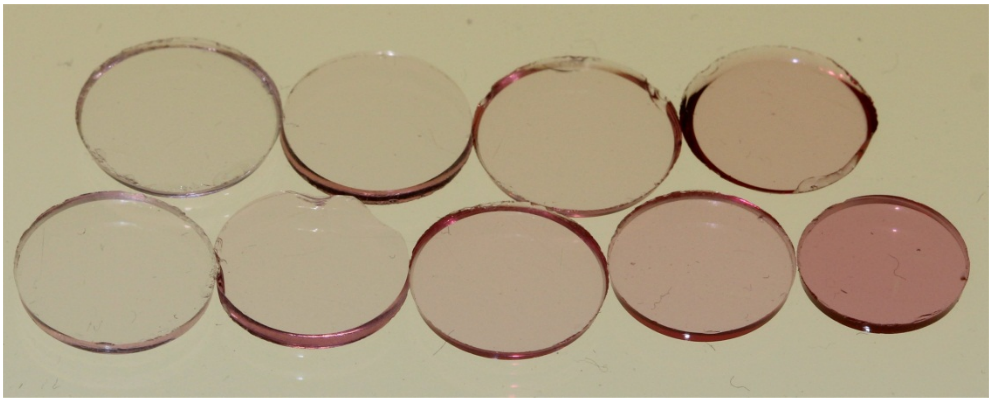

Polished MTEOS glass materials, AuNP-S1 – AuNP-S4 (top) and AuNP-S10 – AuNP-S14 (Bottom)

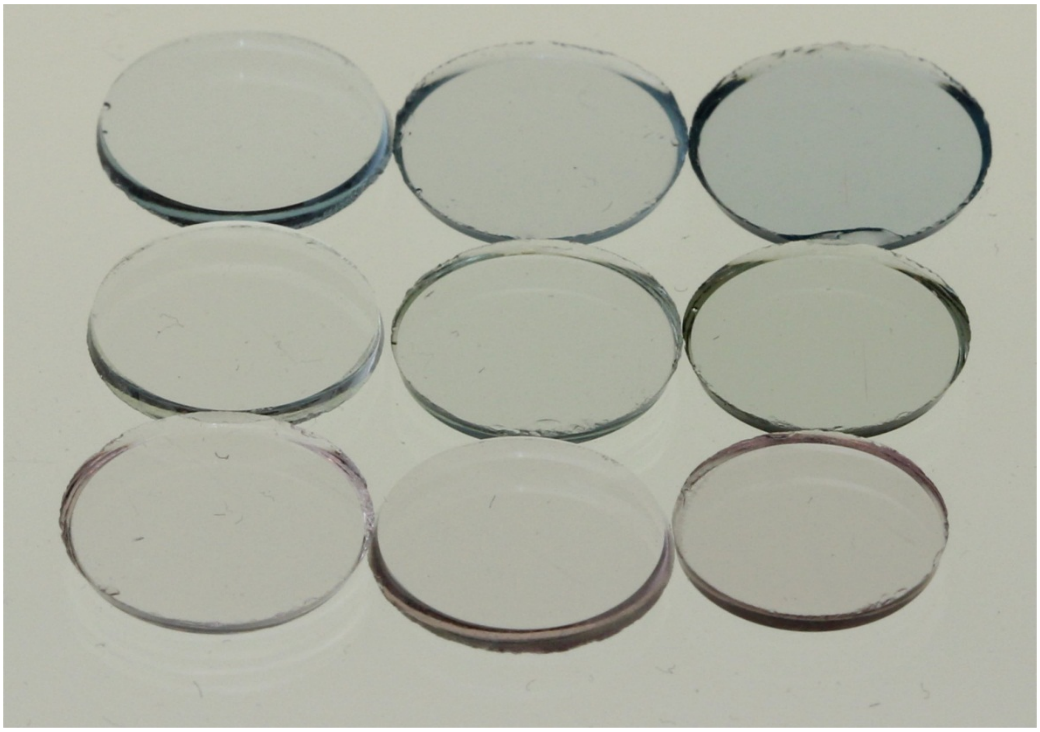

Polished MTEOS glass materials, AuNP-B31 – AuNP-B33 (top), AuNP-B41 – AuNP-B43 (middle) and AuNP-B51 – AuNP-B53 (bottom)

Spectroscopic Ellipsometry

Figure 1 shows the recorded Ψ for sample AuNP-B33 at incidence angles ranging from 0 to 65 degrees, using the collimated beam of 1.5 mm diameter. The full lines in Figure 1 shows how the peak in Ψ develops with increasing incidence angle. It is clear that there is no anisotropy in the absorption for the two orthogonal components of the E-field (s and p-polarization) in the plane, while the anisotropy shows clear signs of a uniaxial system with different absorption in the plane (ordinary component) and perpendicular to the plane (extraordinary component). This behavior can be exemplified by considering a uniaxial substrate, and introducing a weak Lorentzian lineshape in the ordinary component for sample AuNP-B33 with centre energy at 640 nm, and another lineshape centred at approximately 500 nm. Note that the latter position was not fitted, only the amplitude and the broadening, as there appears to be additional structures in the glass host matrix that must be included to reach the required sensitivity in the fit. Furthermore, the main peak appears also to strictly require an assymetrical lineshape, or several Lorentzian lineshapes. The two fitted lineshapes chosen here, only weakly modulates the optical properties of the host matrix described by a dispersion model with parameters similar to those of SiO_2. Figure 2 shows the resulting complex dielectric function, when fitted to only Ψ (or m_{12}) in the range 0-55 degrees. Note that m_{33} and m_{34} does not fit well, which indicate that a more advanced model is needed to capture all the details of the sample, such as e.g. inhomogeneous top and bottom surface layers, however, this fit conveys well the phenomena described by the simplified model introduced by equation (3).

Finally, Figure 3 shows that there is no structure in the recorded Ψ from standard reflection ellipsometry around the plasmon resonances.

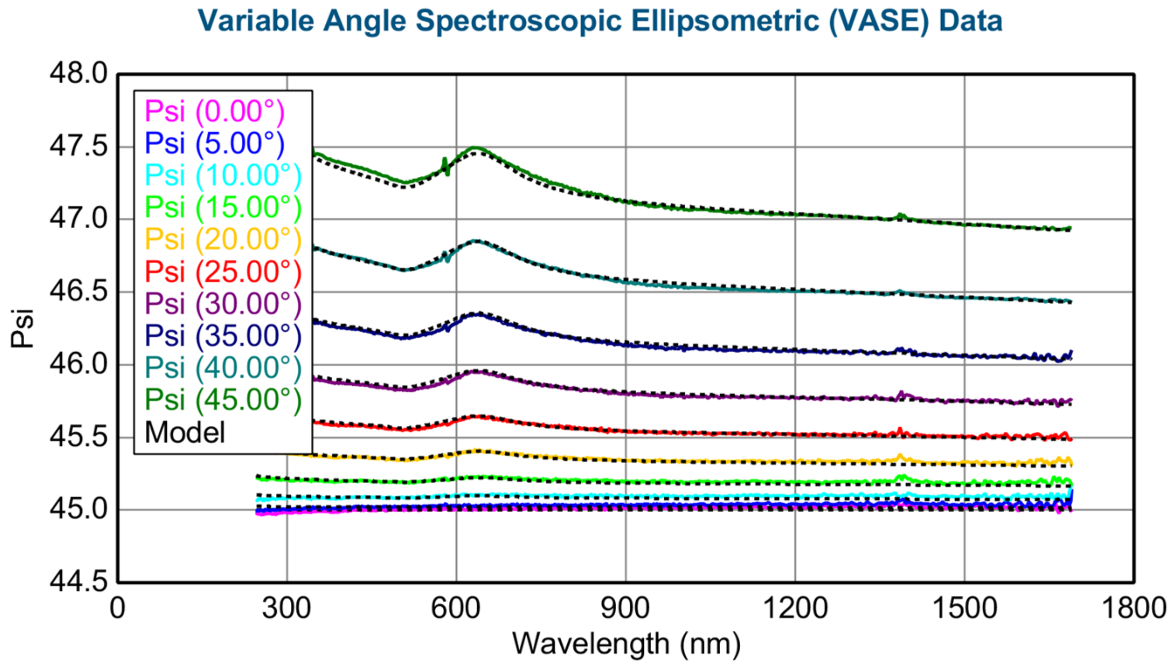

Figure 1. The recorded Ψ for sample AuNP-B33 for incidence angles 0 to 45 degrees in steps of 5 degrees. The full lines show the recorded data, while the black dotted lines are the simulations as a result of the fit.

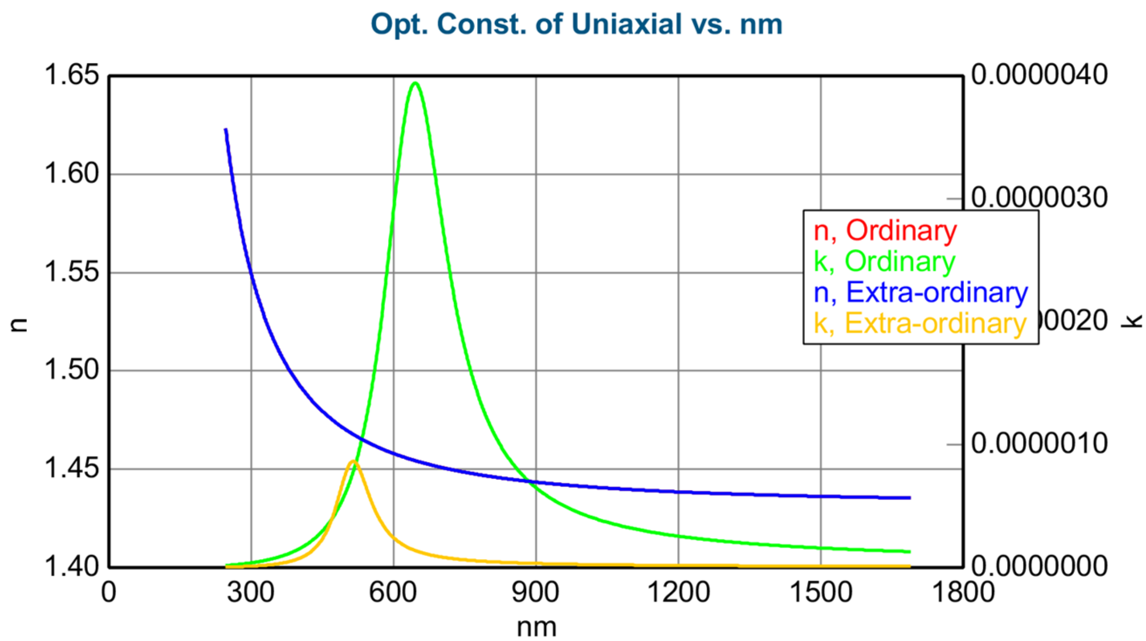

Figure 2. The fitted complex refractive index of the substrate. The two Lorentzian lineshapes in the exctinction coefficients (right axis) of the ordinary component (green line) and extra-ordinary-component (yellow line).

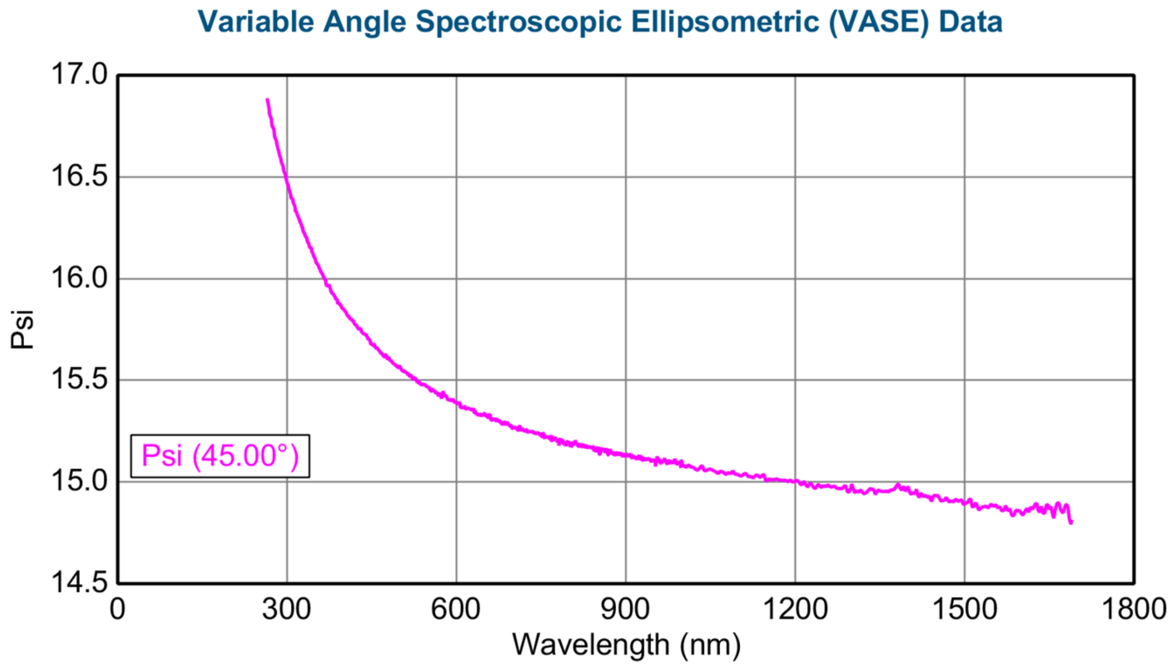

Figure 3. The recorded Ψ for sample AuNP-B33 for incidence angle of 45 degrees.

Linear transmission measurements

The UV-VIS linear transmission measurements show the uniform size distribution of AuNP for the glasses.

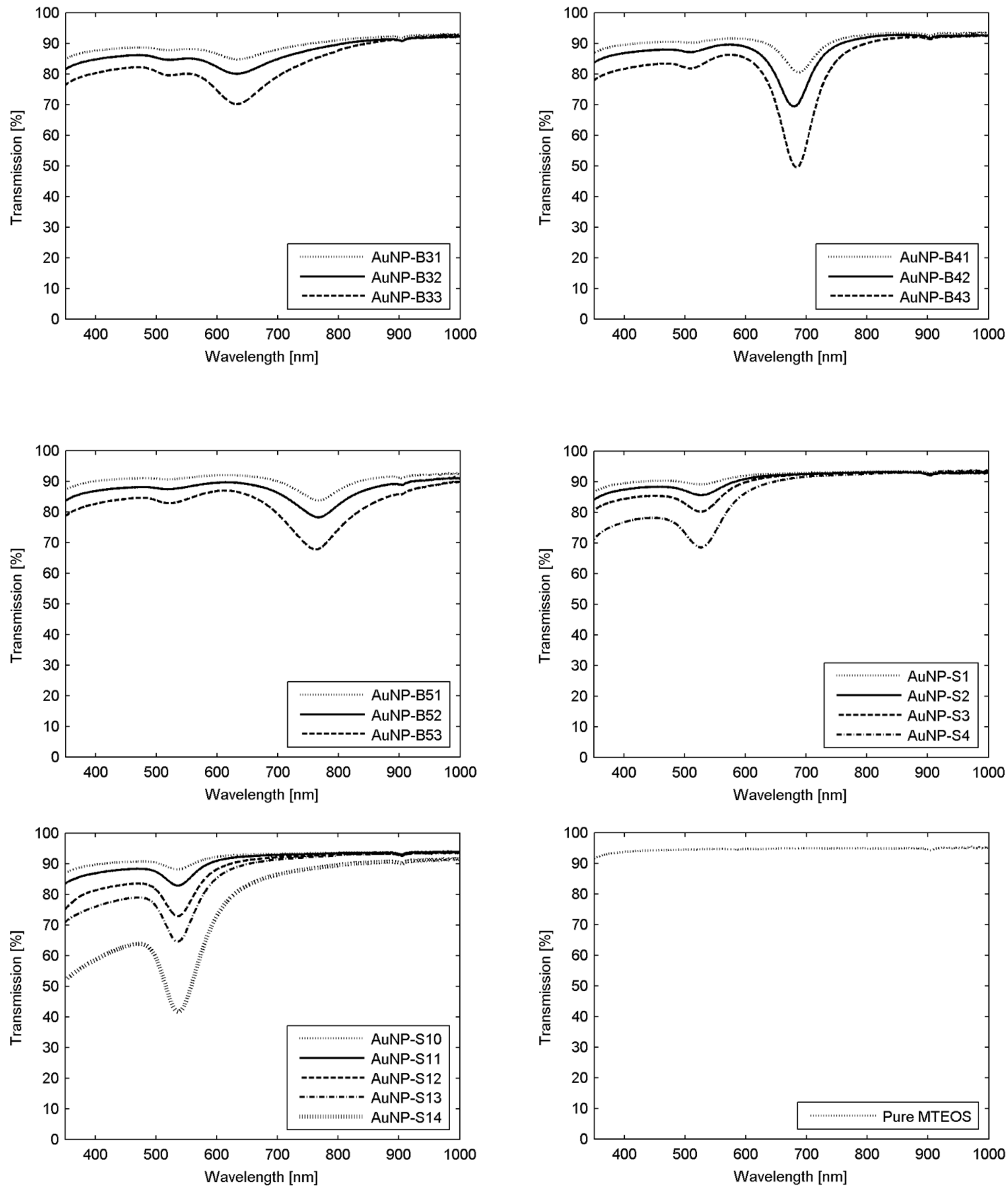

Optical Power Limiting Measurements

Optical power limiting plots for the glasses at 532 nm and 600 nm is presented. For comparison the linear transmission from the UV-VIS measurements are presented in tables.

OPL experiments @ 532 nm AuNP-S1 – AuNP-S4

Material	Transmission @ 532 nm
AuNP-S1	89,2
AuNP-S2	85,7
AuNP-S3	80,4
AuNP-S4	68,9

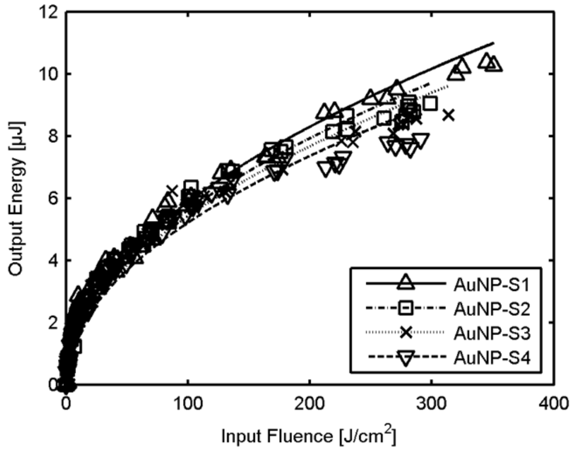

OPL experiments @ 532 nm AuNP-S10 – AuNP-S14

Material	Transmission @ 532 nm
AuNP-S10	88,2
AuNP-S11	83,0
AuNP-S12	73,1
AuNP-S13	64,8
AuNP-S14	42,2

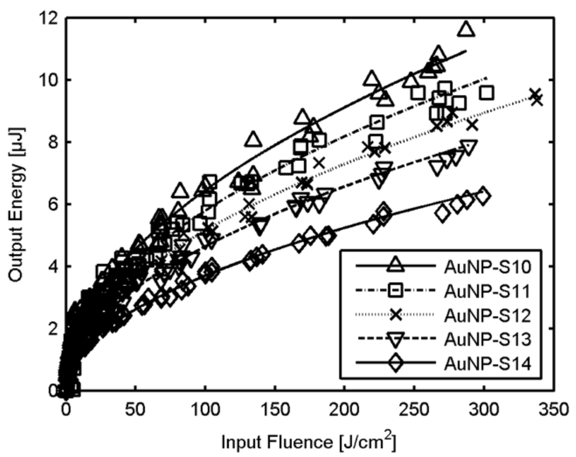

OPL experiments @ 532 nm AuNP-B31 – AuNP-B33

Material	Transmission @ 532 nm
AuNP-B31	87,9
AuNP-B32	84,8
AuNP-B33	79,8

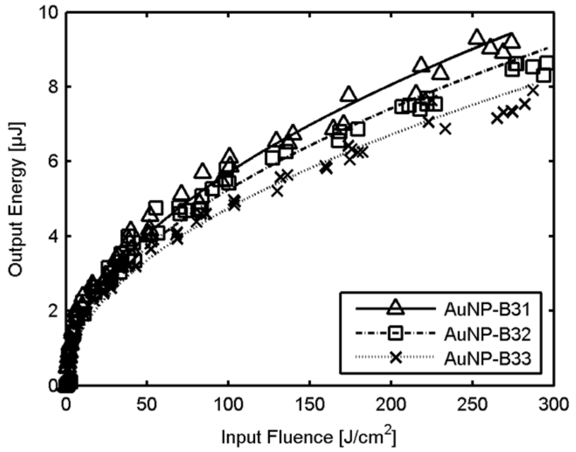

OPL experiments @ 532 nm AuNP-B41 – AuNP-B43

Material	Transmission @ 532 nm
AuNP-B41	90,8
AuNP-B42	88,2
AuNP-B43	83,6

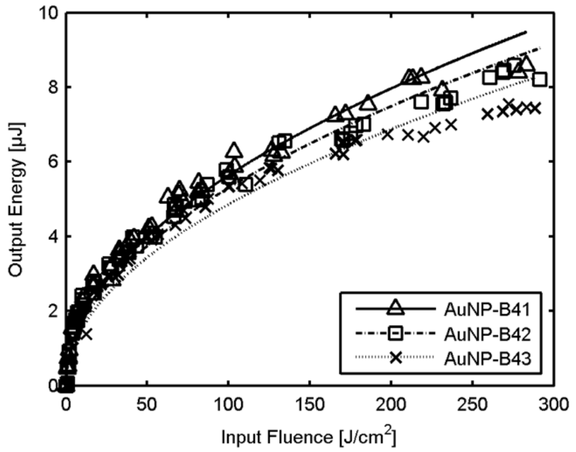

OPL experiments @ 532 nm AuNP-B51 – AuNP-B53

Material	Transmission @ 532 nm
AuNP-B51	90,8
AuNP-B52	87,6
AuNP-B53	83,1

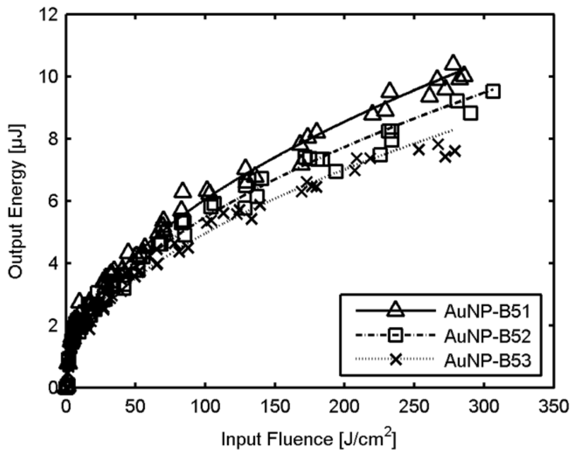

OPL experiments @ 532 nm Pure MTEOS

Material	Transmission @ 532 nm
Pure MTEOS	94,7

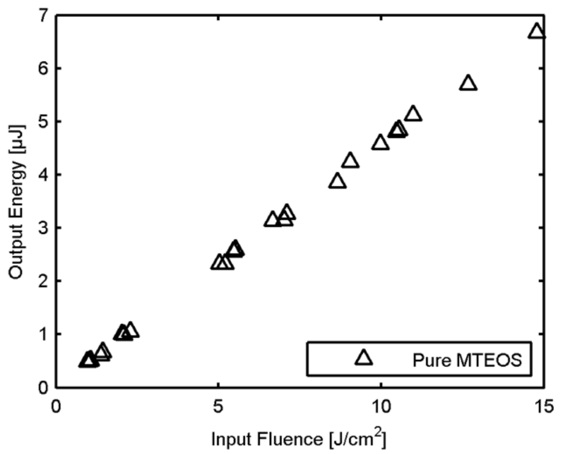

OPL experiments @ 600 nm AuNP-S1 – AuNP-S4

Material	Transmission @ 600 nm
AuNP-S1	92,0
AuNP-S2	91,0
AuNP-S3	89,9
AuNP-S4	86,4

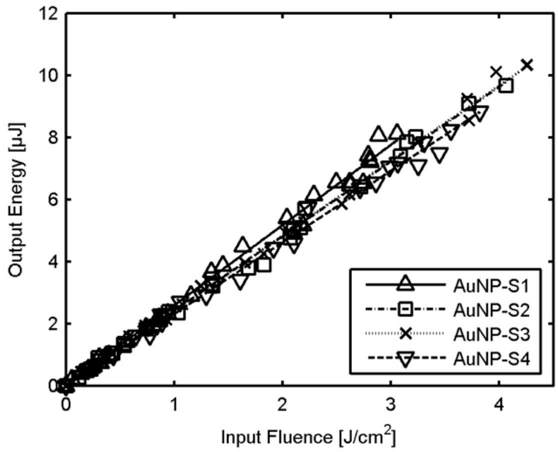

OPL experiments @ 600 nm AuNP-S10 – AuNP-S14

Material	Transmission @ 600 nm
AuNP-S10	92,3
AuNP-S11	91,0
AuNP-S12	88,2
AuNP-S13	85,4
AuNP-S14	73,1

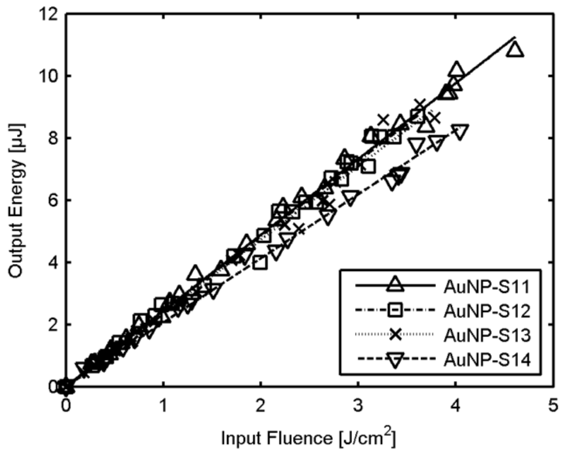

OPL experiments @ 600 nm AuNP-B31 – AuNP-B33

Material	Transmission @ 600 nm
AuNP-B31	86,6
AuNP-B32	82,3
AuNP-B33	74,6

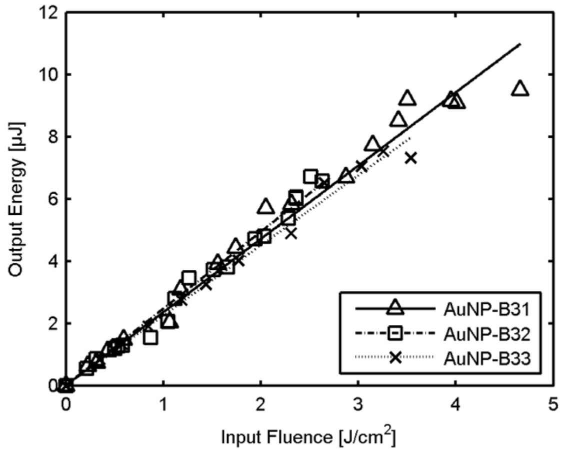

OPL experiments @ 600 nm AuNP-B41 – AuNP-B43

Material	Transmission @ 600 nm
AuNP-B41	91,5
AuNP-B42	88,9
AuNP-B43	85,2

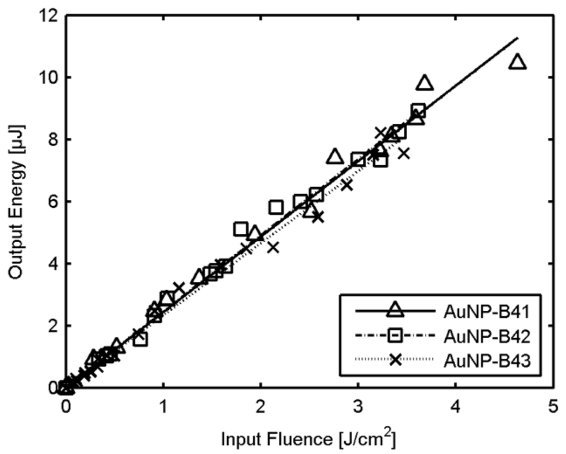

OPL experiments @ 600 nm AuNP-B51 – AuNP-B53

Material	Transmission @ 600 nm
AuNP-B51	92,0
AuNP-B52	89,6
AuNP-B53	86,9

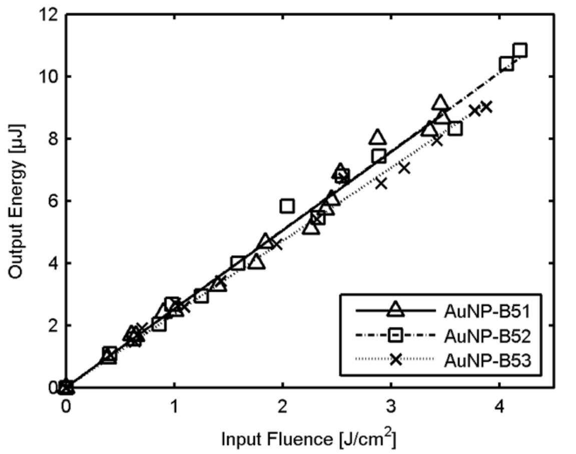

OPL experiments @ 600 nm Pure MTEOS

Material	Transmission @ 600 nm
Pure MTEOS	94,7

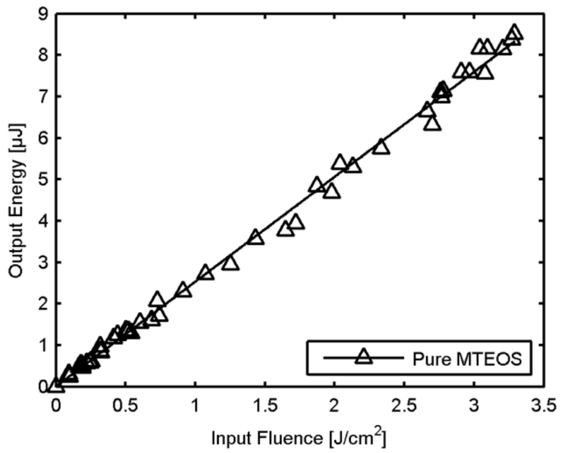

Curve fitting of OPL data

In the article the 532 nm OPL data was curve fitted to $Q_e \approx \eta\sqrt{\Phi}$. No interesting pattern in the varying of η relative to the linear absorption of the glasses at 532 nm was found.

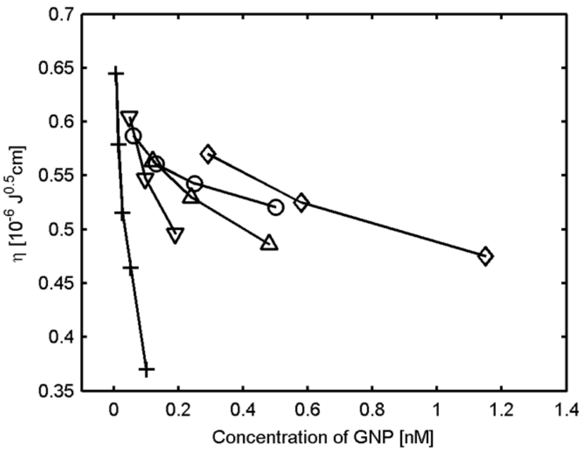

AuNP-S1 – AuNP-S4 (○), AuNP-S10 – AuNP-S14 (+), AuNP-B31 – AuB33 (◊), AuNP-B41 – AuB43 (△), AuNP-B51 – AuB53 (▽).

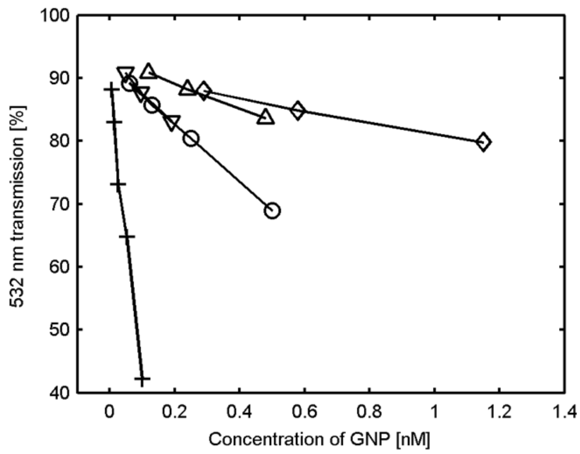

AuNP-S1 – AuNP-S4 (○), AuNP-S10 – AuNP-S14 (+), AuNP-B31 – AuB33 (◊), AuNP-B41 – AuB43 (△), AuNP-B51 – AuB53 (▽).

The curve fitting resulted in a root mean square error of σ for the different glasses.

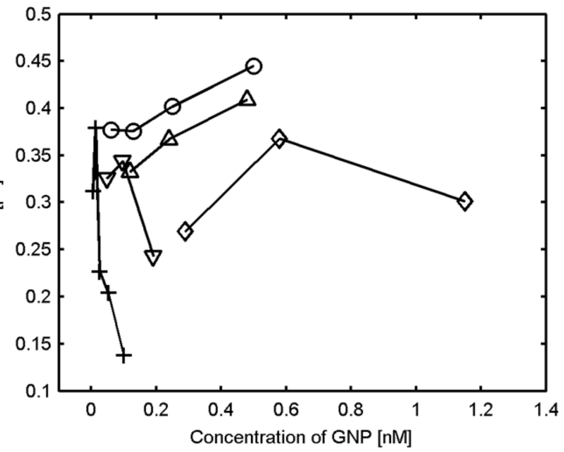

AuNP-S1 – AuNP-S4 (○), AuNP-S10 – AuNP-S14 (+), AuNP-B31 – AuB33 (◊), AuNP-B41 – AuB43 (△), AuNP-B51 – AuB53 (▽).